Industrial Engineering Journal
ISSN: 0970-2555
Volume : 52, Issue 3, March : 2023

STRUCTURAL ANALYSIS OF ALUMINUM A356-T6 AUTOMOTIVE RIM UNDER RADIAL LOAD AND TYRE AIR PRESSURE

Ehthesham uddin Qureshi Assistant Professor, Department of Mechanical Engineering, Deccan College of Engineering & Technology, Hyderabad, Telangana State, India.
Md Musthak Associate Professor, Department of Mechanical Engineering, Deccan College of Engineering & Technology, Hyderabad, Telangana State, India. (Corresponding author Email: musthak.mech@gmail.com)

Abstract: *Automotive wheels have evolved over the decades from early spoke designs of wood and steel, carryovers from wagon and bicycle technology, to flat steel discs and finally to the stamped metal configurations and modern cast and forged aluminum alloys rims of today's modern vehicles. The wheel of an automobile vehicle is an important part of the vehicle, its role is vital from safety point of view. If a wheel rim is used in severe operating conditions such as racing or rallying; hidden damage may occur. This may result in a fetal accident or sudden wheel rim failure whilst the vehicle on road. Therefore it is very necessary to test and analyze the wheel-rim. Wheels are clearly safety related components and hence fatigue performance and the state of stress in the rim under various loading conditions are prime concerns. Further, wheels continue to receive a considerable amount of attention as part of industry efforts to reduce weight through material substitution and down gauging. Although wheels are loaded in a complex manner and are highly stressed in the course of their rolling duty, light weight is one of the prime requirements, hence cast and forged aluminum alloys are essential in the design. Light aluminum alloy wheels enjoy a great popularity at present. For many consumers, a perceived exclusivity is a predominate factor, and these wheels are even considered as status symbols. The necessity to improve fuel consumption has caused many motor car manufacturers to break new ground in their vehicle design. Rounded surfaces have also clearly demonstrated that a smooth outer wheel surface gives a further reduction in air resistance.*

In recent years, the procedures for wheel rim testing have been improved by a variety of experimental and analytical methods for structural analysis. Within the past 10 years, durability analysis (fatigue life predication) and reliability methods for dealing with the variations inherent in engineering structures have been applied to the automotive wheels. In this context, stress and deflection analysis of automotive rim under radial load and tyre air pressure is important. As such, in this paper, stress and deflection analysis of wheel – rim under radial load and tyre air pressure has been carried out using finite element method. Several methodologies for modeling the effect of the vehicle weight as it is transferred to the rim are presented in this paper. Under radial load the rim tends to ovalize about the point of contact, with a maximum displacement occurring at the location of the bead seat. Radial loading accounts for and acceleration factor of 2.2. Analysis was based on SAE (Society of Automotive Engineers) specifications. The inside bead seat deflects the greatest and is prone to loss of air pressure due to the dislodgment of the Tyre to the rim.

Keywords: Automotive wheel-rim, Finite Element Method, Radial load, Tyre air pressure.

Industrial Engineering Journal
ISSN: 0970-2555
Volume : 52, Issue 3, March : 2023

INTRODUCTION

Historically, successful designs arrived after years of experience and extensive field testing. Since the 1970's several innovative methods of testing well aided with experimental stress measurements have been initiated [1]. In modern years, the procedures have been improved by a variety of experimental structural analysis by using strain gauges and analytical structural analysis by using finite element methods. In last decades, durability analysis (fatigue life prediction) and reliability methods for dealing with the variations inherent in engineering structure has been considered for automotive wheels. Wheels are clearly safety related components and hence fatigue performance and the state of stress in the rim under various loading conditions are prime concerns.

Material Properties

Further, wheels continue to receive a considerable amount of attention as part of industry efforts to reduce weight through material substitution and down gauging. Although wheels are loaded in a complex manner and are highly stressed in the course of their rolling duty, light weight is one of the prime requirements, hence cast and forged aluminum alloys are essential in the design. Light aluminum alloy wheels enjoy a great popularity at present. For many consumers, a perceived exclusivity is a predominate factor, and these wheels are even considered as status symbols. The necessity to improve fuel consumption has caused many motor car manufacturers to break new ground in their vehicle design. Rounded surfaces have also clearly demonstrated that a smooth outer wheel surface gives a further reduction in air resistance. With all this attention to automotive wheels, the consumer still expects wheels to be indestructible and highly reliable automotive components. In casting alloys collection, A356 aluminum is a typical material for automobile applications. Unlike wrought alloys, cast aluminum has a different designation system. In this article, we'll focus on A356 (A356-T6) aluminum alloy, the material properties of Aluminum A356-T6 is shown in table 1.

Table 1: Material Properties of Aluminum A356-T6

Properties	Values
Molar Mass	26.98 g mol^{-1}
Density	2750 Kg m^{-3}
Specific heat capacity	1047 J Kg^{-1} K^{-1}
Dynamic viscosity	0.0025 Kg $m^{-1}s^{-1}$
Thermal conductivity	180 $Wm^{-1}K^{-1}$
Thermal co-efficient of expansion	$4x10^{-5}$ K^{-1}

Loading Methodologies

In this paper several methodologies for modeling the effect of the vehicle weight as it is transferred to the rim are presented. Methods explained are referenced in the published literature and analogies taken from thick ring theory in stress analysis in the development of loadings on links and eye-bars. As stated, the modeling of the tyre on the rim is extremely complex and involves non-linear analysis on tyre portion coupled with linear static stress analysis on rim. The interface of the two components would be achieved by the use of gap or contact elements. This work has been done at The Goodyear tyre and Rubber Company. Results indicate that the loading shape is in the form of a cosine function about a central angle of approximately 30^{o} from either side of the point of contact with the ground.

Others assumed this 30^{o} angle is developed from the contact patch geometry of the tyre. Meaning that when the Tyre is loaded there is flat spot at the point of contact with the ground, this is so called contact patch, and the length of this patch is then converted to an equivalent angle swept by the bead seat area in contact with the rim. At the other end, the bead seat areas tend to be pulled away from the rim, so no loading is present in the areas or is considered negligible. Finally a method proposed assumes the area in contact with

the rim spans half of the tyre or 90º symmetrical about the point of loading. The loading method is similar to a cylindrical bar in a clevis, assuming no gap exists. This method is coined the eye-bar loading method. All methods are explained in this paper.

Eye-Bar Analogy

Comparison of a round rod in an eye bar under equilibrium of forces is shown in Figure 1 [2]. The figure explains r is the radius of the hole, W is the load imparted, θ is the angle and q_{max} is the maximum point load. The horizontal components of q are in balance with each other.

The vertical forces can be related to the external load, W which is expressed as follows:

$$W = 2 * r \int_0^{\pi/2} q * \cos\theta \, . \, d\theta \ldots\ldots\ldots\ldots (1)$$

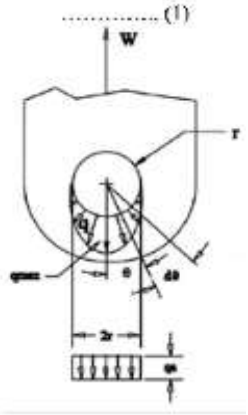

Figure 1: Eye-bar loading

By defining q = q_{max}*cos θ and substituting into the equation (1),

$$W = 2 * r \int_0^{\mu/2} q_{max} * \cos^2\theta \, . \, d\theta$$

$$W = 2 * r * q_{max} \left[\frac{\theta}{2} + \frac{Sin2\theta}{4} \right]_0^{\pi/2}$$

$$W = 2 * r * q_{max} \left[\left(\frac{\pi/2}{2} + \frac{*Sin2*\pi/2}{4} \right) - (0) \right]_0^{\pi/2}$$

$$\therefore q_{max} = \frac{2*W}{\pi * r} \qquad \ldots (2)$$

q_{max} is in unit load N/mm and r is the radius of the bead seat. Normally this radius is assumed to be nearly equal to the pin radius. Dividing by q_{max} by its width of the eye-bar cross section gives the compressive stress based on the above model. With W = 3113 N and r = 202 mm.

$$\therefore q_{max} = \frac{2*3113}{\pi * 202} = 9.81 N/mm$$

Dividing q_{max} by the bead seat width, b=19.8 mm yields the compressive pressure load on the seat. In this application, the calculated result is 4955 kPa.

Analysis under Radial Load

The whole weight of automotive vehicle is balanced with a vertical reaction force from the road through the tyre. This load constantly compresses the wheel radially. While the vehicle is running, the radial load becomes a cyclic load with the rotation of the wheel. Hence, the evaluation of wheel fatigue strength under radial load is an important performance characteristic for structural integrity. According to the SAE

Industrial Engineering Journal
ISSN: 0970-2555
Volume : 52, Issue 3, March : 2023

specification, a wheel should maintain structural integrity without any cracks or plastic deformation for more than 4 x 10^6 rotations under a radial load. The radial load, Q, is expressed by:

$$Q = S_r * W \quad \dots (3)$$

Where, S_r means acceleration test factor (S_r = 2.2) and W means maximum tyre load. For this application W=7157 N, thus Q = 15745 N.

Under a radial load, the strength of the rim usually determines the fatigue life of a wheel, so the stress evaluation is mainly focused on the radial load. In this analysis, the contact condition between the discs spoke flange and the rim well is assumed to be tightly closed. The contact area is modeled by one element with the summed thickness of the disc and the rim.

In an actual wheel, since a radial load is applied to the wheel on the bead seats with the tyre, the distributed pressure is loaded directly on the bead seats of the model.

The pressure is assumed to have a cosine function distribution mode within a central angle of 40^0 in a circumferential direction as shown in Figure 2.

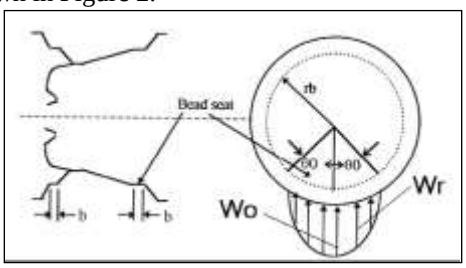

Figure 2: Radial Loading Schematic

The 40° was chosen based on previous literature, in which some determined this angle by strain gauge experiments or some researchers assuming the angle from the contact patch area. Using the idea of the contact patch width corresponds to the area of contact over the bead seats as shown in Figure 3.

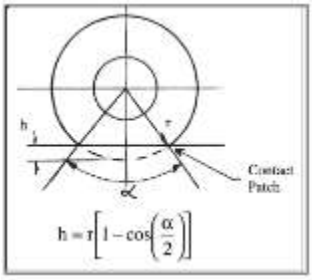

Figure 3: Contact Patch Schematic

By using the cosine function accordingly, the distributed pressure, W_r, is given by the following equation:

$$W_r = W_o * \cos\left(\frac{\pi}{2} * \frac{\theta}{\theta_o}\right) \quad \dots (4)$$

The total radial load W is calculated by using Equation 5 as follows.

$$W_r = b \int_{-\theta_0}^{\theta_o} W_r * r_b . d\theta \quad \dots (5)$$

$$W_r = b \int_{-\theta_0}^{\theta_o} W_o * r_b * \cos\left(\frac{\pi}{2\theta_o} * \theta\right) d\theta$$

$$W_r = b * W_o * r_b * \frac{1}{\left[\frac{\pi}{2\theta_o}\right]} * \sin\left(\frac{\pi}{2} * \frac{\theta}{\theta_o}\right)_{-\theta_0}^{\theta_o}$$

Industrial Engineering Journal
ISSN: 0970-2555
Volume : 52, Issue 3, March : 2023

$$W_r = 4 * b * r_b * \theta_o * \frac{W_o}{\pi}$$

$$W_o = \frac{W_o * \pi}{b * r_b * 4 * \theta_o} \quad \ldots (6)$$

With b=19.8 mm, W=10.4 kN, r_b=202 mm, yields W_0 = 2045 kPa. Where, r_b is the radius of the bead seats and b is the total width of the bead seats. In this analysis, the total radial load W = 15745 N is applied to the model, and the magnitude of the load is the same as applied to the actual wheel during strain measurements.

In this stress measurement experiment, the wheel is assembled with a Goodyear Eagle aqua steel Tyre (P22560R16) which is inflated to a pressure of 241 kPa, and pressed against a flat plate with a load of 3113N. Strain gauges are attached to the wheel in circumferential direction. The central angle 0^0 of the pressure distribution is 80 degrees, which is determined from previous researchers [3] distribution of the rim flange.

Pressure is applied to two bead seats on the inboard side and the outboard side. In detail, half of the pressure on the inboard side is applied to the inboard rim flange, and the other half is applied to the inboard bead seat. The reason for this is that the inboard rim flange deflects easily due to the long inboard rim leg, and so it is susceptible to loading from the Tyre. The loading condition described above is determined from a comparison between the measured stress of the rim and the calculated stress under some tentative loading conditions.

The optimum dividing ratio of the applied load on the bead seat versus the applied load on the rim flange is thought to vary according to the contact condition between the Tyre and the rim. This, in turn, is affected by such factors as Tyre type (bias or radial), the Tyre air pressure, the reinforcement structure of the Tyre and the type of the rim [4]. In actual modeling the locations along the circumference were identified as element numbers (node numbers) and corresponding angle.

Analysis under Tyre Air Pressure

Tyre air pressure is a constant load with no relation to the rotation of the wheel.
However, the induced stress on the rim due to inflation pressure only, is comparatively small. In actual wheel usage, the cyclically varying stress due to the bending moment or the radial load is superimposed on the constant stress generated by the Tyre air pressure. The Tyre air pressure is loaded on the axi-symmetrically shaped rim. In a three dimensional analysis using the mesh subdivision in Figure 4, the induced stress of the non-axi-symmetrically shaped disc was negligible, so an axi-symmetric analysis is sufficient for the stress calculation under the Tyre air pressure.

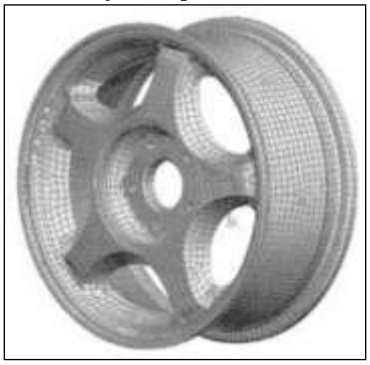

Figure 4: Finite element model

The mesh subdivision used is the axi-symmetric one shown in Figure 5. The element used is an axi-symmetric three node element.

So, from a structural point of view, it is necessary to precisely evaluate the stress induced by the Tyre air pressure. The Tyre air pressure is loaded on the axi-symmetrically shaped rim.

The induced stress of the non-axi-symmetrically shaped disc was negligible, so an axi-symmetric analysis is sufficient for the stress calculation under the Tyre air pressure. The mesh subdivision used is the axi-symmetric one shown in Figure 5.

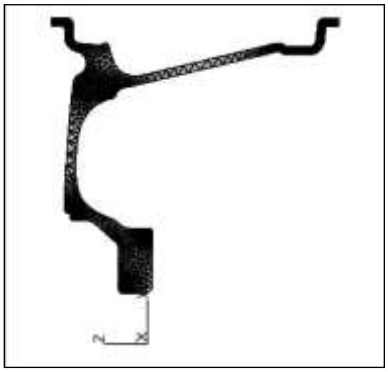

Figure 5: Axis-symmetric model

The element used is an axi-symmetric three-node element. The Tyre air pressure is applied not only directly to the rim outer side but also indirectly to the rim flange. The later load, which is directed in an axial direction, is generated by the air pressure pressing on the Tyre side wall. This load varies according to the type of Tyre, the aspect ratio of the cross section of the Tyre and the reinforcement structure of the Tyre. In this study, the load is calculated by considering the profile of the cross section of the Tyre and assembly shown in Figure 6, the axial component of the force W_p which results from the inflation of the Tyre is calculated by [4] the following equation

$$W_p = \pi\left(a^2 - r_f^2\right)P_o \qquad \ldots (7)$$

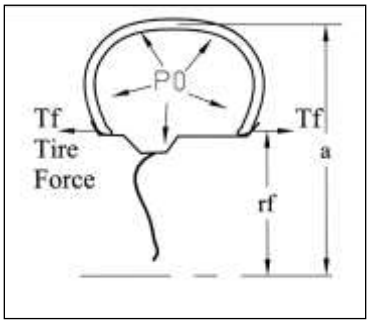

Figure 6: Tyre force schematic

Where, a, is the design radius of the Tyre and r_f is the radius of the loading point on the rim flange. Because the axial load is supported by the tread of the Tyre and the rim flange, approximately a half of the load is assumed to be loaded on each part. So, the load on the circumferential unit length of the rim flange is calculated by the force, T_f, expressed as the following

$$T_f = \frac{W_p}{2*2*\pi*r_f} = \left(a^2 - r_f^2\right)\frac{P_o}{4*r_f} \qquad \ldots (8)$$

Applying, this equation using P_0 = 241 kPa, r_f = 0.2208 m, a = 0.3397 m, yields T_f = 500 N. For 117 kPa, T_f = 251 N, at 0 kPa, T_f = 0 N. The applied air Tyre pressure in this study will vary from 0, 117, 241 and 303 kPa (axis symmetric only). This equivalent technique was compared to a standard pressure loading technique for the axis symmetric model.

Axi-symmetric elements

The deformation of the wheel due to varying air pressure is shown in Figure 7.

This figure shows the general deformed and undeformed shape due to inflation only. In these models the rim flange pressure is applied using pressure loading as defined in ANASYS 8.0 by making this surface a unique color. Pressure varied from 303, 241 and 117 kPa, with 303 kPa being maximum operating pressure, 241 kPa is the normal operating pressure, and 117 kPa is half inflated pressure for the Tyre.

The rim flanges are deflected in the axial direction by the air pressure acting on the Tyre side wall, and also in direct contact with the rim. Due to the geometry in the rim, the inboard side on the rim undergoes bending due to the offset in the rim, when compared with the other end. Results show that the area of highest stress in the axi-symmetric elements is at the well, as predicted in the literature review. High stresses are also seen in the rim flange area, as well as the transition area where the bead seat riser is on the inboard side of the rim.

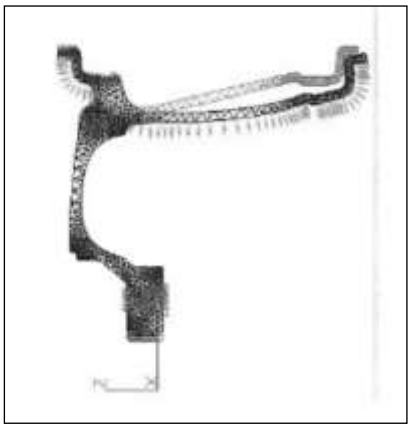

Figure 7: Deformed Axi-symmetric Model

These general locations and recorded stresses compared favorably with other referenced literature [5]. Location of high stresses in the well area is of major concern for welded rims. Typically, the disc is welded to the rim at the well area. Residual stress causes additional stress or possible micro structural cracks to the rim. When comparing effects of air pressure, stresses dropped in a linear relation to the applied pressure. Deflections in the rim were negligible (0.29 mm). Deflection results are similar to results obtained from other researches [5] and internal studies at the Goodyear Tyre and Rubber Company. The next step was to compare point load models for pressure effects developed by other authors [5, 6] with direct pressure effects using finite element methods. Results at 241 kPa were compared with Morita [4] to ensure the convergence of the software and the model that was developed. Maximum principal stress of 6412 kPa was calculated at the round hump location as shown in Figure 9. Figure 9 compares the outside surface to the inside or Tyre side surface at 241 kPa inflation pressures. The cut section of the disc section geometry of the model was taken through the spoke area. This geometry will results in a variation of stress values when compared to the full three dimensional hexahedral finite element model. Meshing technique also plays an important role in the results. Other locations of high stress magnitudes are the bead seat inside surface. This would be the surface of contact with the Tyre. Loss of air pressure results in lower stresses in this area, hence lower holding forces.

The stresses were quite low as expected for air pressure only. The analysis was repeated at 303 kPa (radial load test pressure per SAE [7]), and 117 kPa loading. Results are shown in Figures 8 through 11. A comparison is made in Figure 11 for varying air pressure effects. Plotting the pressure versus the stress a direct linear relationship is verified. Figure 8 plots the principal stress for the inside and outside surface of the wheel rim face as a function of 303 kPa inflation pressure. In this case the outside surface is considered the side of the Tyre cavity side of the rim and is plotted in the dashed lines. This outside surface contains the highest principal stresses on the rim and occurs at the well.

In contrast the highest principal stresses on the inside surface occurs at the hump. The same trend can be seen in Figures 9 and 10 showing the 241 kPa and 117 kPa inflation pressures. In all three cases, peak

Industrial Engineering Journal
ISSN: 0970-2555
Volume : 52, Issue 3, March : 2023

stresses did not shift and the reduction in stresses are linear when compared to the reduction in Tyre inflation pressure.

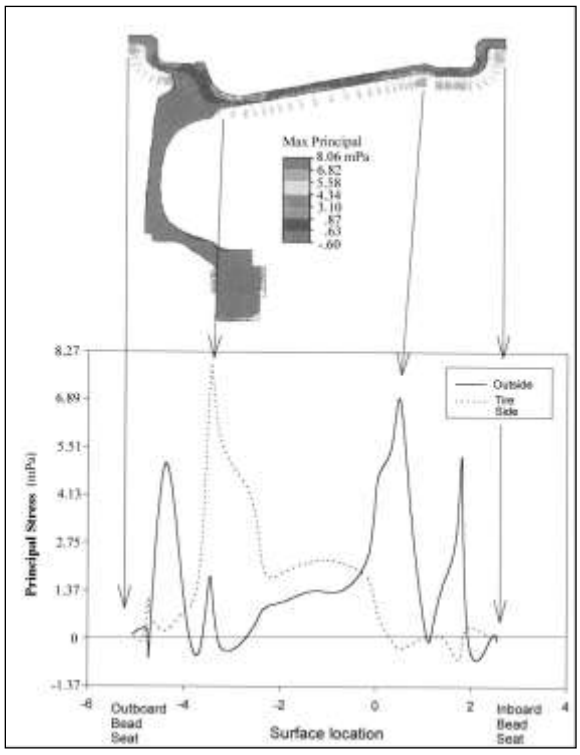

Figure 8: Influence of Inflation Pressure for the Axis symmetric Model at 303 kPa

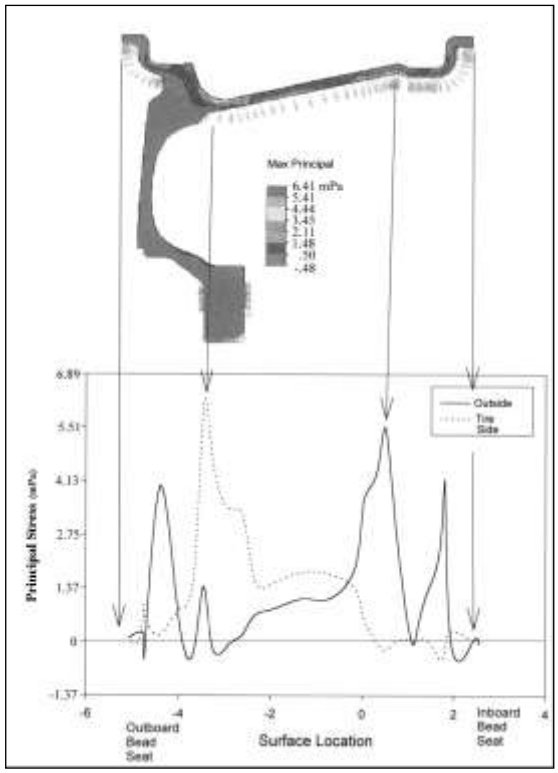

Figure 9: Influence of Inflation Pressure for the Axis symmetric Model at 241 kPa

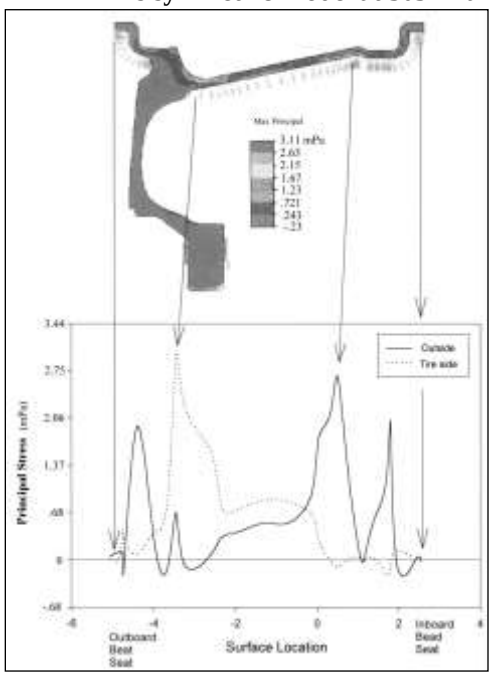

Figure 10: Influence of Inflation Pressure for the Axis symmetric Model at 117 kPa

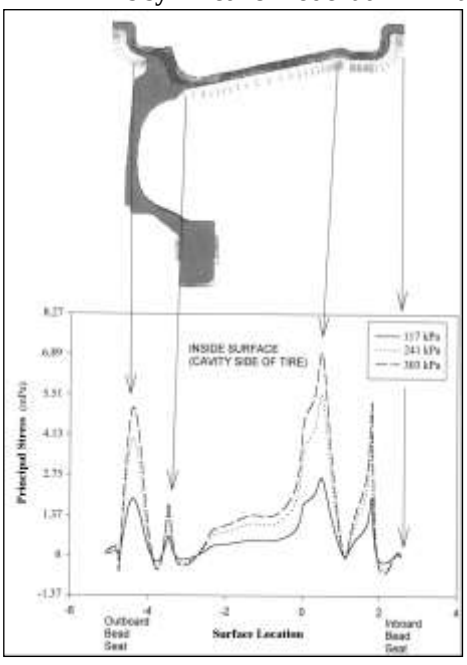

Figure 11: Influence of Inflation Pressure for the Axis symmetric Model

CONCLUSION

Based on this study, using the finite elements technique the influence of inflation pressure on distribution of stress and resultant displacement in and automobile rim made from aluminum alloy A356-T6, it is observed that the various methods of applying the radial load have been established and all take a cosine function form, application of the cosine function is dependent on tyre construction. The Effect of inflation pressure can be modeled as an equivalent load on the bead seat flange and Inflation pressure does have a direct effect on the state of stress in an automobile rim under the influence of a load of the maximum tyre rating, coupled with and acceleration factor. Under radial load the rim tends to ovalize about the point of contact, with a maximum displacement occurring at the location of the bead seat. Radial loading accounts for and acceleration factor of 2.2. Analysis was based on SAE (Society of Automotive Engineers) specifications. The inside bead seat deflects the greatest and is prone to loss of air pressure due to the dislodgment of the Tyre to the rim.

REFERENCES

1. **Krause, G., and Mahnig, F.,** "A comprehensive Method for Wheel Testing by Stress Analysis," SAE Technical Paper Series #760042, 1976.
2. **Blake, A.,** "Practical Stress Analysis in Engineering Design," McGraw-Hill, pp. 363- 367, 1990.
3. **Kawashima, H., and Ishihara, K.,** "Stress Evaluation of Automotive Steel Road Wheel Under Radial Load," Nippon Kikai Gakkai Ronbunshu, C Hen, Vol. 55, No. 513, pp. 1254-1258, 1989.
4. **Hoemsen, R.,** "Structural Design of Agricultural Wheels," American Society of Agricultural Engineers #84-1558, 1984.
5. **Kawashima, H., and Ishihara, K.,** "Stress Evaluation of Automotive Steel Road Wheel Under Radial Load,", Nippon Kikai Gakkai Ronbunshu, C Hen, Vol. 55, No. 513, pp. 1254-1258, 1989.
6. **Woods, R.,** "Finite Element Analysis Case Study: Wheel Optimization," University of Dayton, 1988.
7. **Plummer, H., Simmons, R., Ocobock, R. Honey, T., and Peck, M.,** "Study of Factors Affecting Corrosion of Aluminum alloy Automotive Wheels," Proceedings of the 51st Annual Meeting Microscopy Society of America, Code 19435, pp.1182-1183, 1993.